High-Precision Spectroscopy of the Forbidden $2\,^3S_1 \rightarrow 2\,^1P_1$ Transition in Quantum Degenerate Metastable Helium

R. P. M. J. W. Notermans and W. Vassen*

LaserLaB, Department of Physics and Astronomy, VU University Amsterdam, De Boelelaan 1081, 1081 HV Amsterdam, Netherlands

(Received 27 March 2014; published 25 June 2014)

We have measured the forbidden $2\,^3S_1 \rightarrow 2\,^1P_1$ transition at 887 nm in a quantum degenerate gas of metastable ^{4}He atoms confined in an optical dipole trap. The determined transition frequency is 338 133 594.4 (0.5) MHz, from which we obtain an ionization energy of the $2\,^1P_1$ state of 814 709 148.6 (0.5) MHz. This ionization energy is in disagreement by $> 3\sigma$ with the most accurate quantum electrodynamics calculations available. Our measurements also provide a new determination of the lifetime of the $2\,^1P_1$ state of $0.551\,(0.004)_{\mathrm{stat}}\,(^{+0.013}_{-0.000})_{\mathrm{syst}}$ ns, which is the most accurate determination to date and in excellent agreement with theory.

DOI: 10.1103/PhysRevLett.112.253002 PACS numbers: 32.30.-r, 05.30.Jp, 31.30.J-, 42.62.Eh

QED is one of the most thoroughly tested theories in physics. From QED theory and accurate measurements, the fine structure constant [1,2], the Rydberg constant [3], nuclear charge radii [4,5], and the electron mass can be deduced [6]. It can also provide accurate ionization energies for one- and two-electron atoms. To test QED, both highly accurate calculations and high-precision experimental data are required. Few-body systems such as the hydrogen atom and helium atom are candidates that fulfill both criteria. Testing and applying QED in these systems has led to surprising results in recent years. An example is the 7σ discrepancy in the proton size derived from muonic hydrogen Lamb shift measurements and the accepted CODATA value, also referred to as the proton size puzzle [4,7]. Recent measurements of the helium $2\,^3S \rightarrow 2\,^1S$ transition at 1557 nm [5] and the $2\,^3S \rightarrow 2\,^3P$ transitions at 1083 nm [8] disagree by 4σ in the determination of the helium isotopic nuclear size difference. These measurements provide a unique comparison with nuclear size measurements in the muonic helium ion, developed to help solve the proton size puzzle [9]. Recent experiments with trapped highly charged heliumlike ions also show a significant discrepancy with QED theory, 3σ for Ti^{20+} and growing as Z^3 [10].

In particular, for the low-lying states with low angular momentum, accurate measurements of the ionization energies (IE) in helium have allowed stringent tests of two-electron QED [5,8,11–15]. A schematic overview of the lowest states of helium together with transition wavelengths mentioned in this Letter are shown in Fig. 1. In comparing the experimentally determined IE to QED calculations, a discrepancy of 6.5 (3.0) MHz in the $2\,^1P_1$ IE was identified by Drake and Pachucki [16–18]. This discrepancy is based on a measurement of the $2\,^1P_1 \rightarrow 3\,^1D_2$ transition frequency with 3 MHz accuracy by Sansonetti and Martin in 1984 [19]. As the QED calculation of this IE is accurate to 0.4 MHz [18], a more accurate measurement should be able to determine whether this discrepancy still stands. Recently, two new determinations of the $2\,^1P_1$ IE were reported by Luo *et al.* based on measurements of the $2\,^1S_0 \rightarrow 2\,^1P_1$ [20] and $2\,^1P_1 \rightarrow 3\,^1D_2$ [21] transition frequencies. As these transitions are electric dipole allowed, the measurements could be done using saturated absorption spectroscopy in a rf discharge cell. The extracted ionization energies for the $2\,^1P_1$ state disagree with QED theory at the 3.5σ level.

In this work we report the direct measurement of the forbidden $2\,^3S_1 \rightarrow 2\,^1P_1$ transition at 887 nm in a quantum degenerate gas (QDG) of metastable $2\,^3S_1$ state helium (denoted ^{4}He*, lifetime ≈7800 s) atoms confined in an optical dipole trap (ODT). The advantage of performing spectroscopy in an ODT is the ability to probe very weak

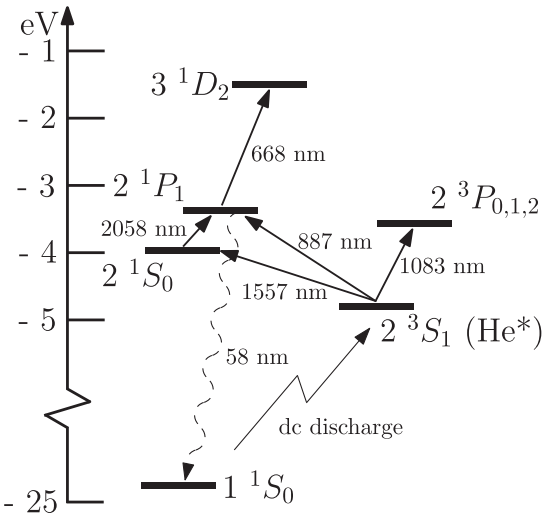

FIG. 1. Schematic overview of the energies of the lowest levels in ^{4}He (with respect to the ionization limit) and the transitions that are mentioned in this work. The $2\,^3S_1 \rightarrow 2\,^3P_2$ transition at 1083 nm is used for laser cooling and trapping.

transitions and the simultaneous reduction and characterization of systematic effects to the kHz level [5]. As the theoretical natural linewidth of this transition is 287 MHz [22], the accuracy of our measurement is limited by statistics rather than by systematic effects. Combined with the accurately known IE of the $2\,^3S_1$ state, this measurement of the transition frequency enables a determination of the $2\,^1P_1$ IE.

The measured line shape of the transition allows for an accurate determination of the lifetime of the $2\,^1P_1$ state. This method does not require the branching ratios of decay channels, which is the main problem in fluorescence measurements of the lifetime [23], and the only dominant broadening effect in our experiment can be calculated using the optical Bloch equations.

The $2\,^3S_1 \rightarrow 2\,^1P_1$ transition is forbidden as it violates conservation of spin. Because of a small mixing of the $2\,^1P_1$ and $2\,^3P_1$ states [24], the electric dipole transition has an Einstein A coefficient of 1.4423 s^{-1}, which is 7 orders of magnitude weaker than regular dipole-allowed transitions in the helium atom [25]. Therefore, to our knowledge, this transition has never been observed before. In order to obtain a good signal with reasonable laser power, the atoms need to be probed on a time scale of about 1 s, and we achieve this by trapping a QDG of $^4He^*$ atoms in an ODT. For this we use the same experimental setup as used to measure the doubly forbidden $2\,^3S \rightarrow 2\,^1S$ transition [5]. We produce a QDG consisting of a thermal gas and a Bose-Einstein condensate (BEC) in a crossed-beam ODT, which is created using an NP Photonics fiber laser operating at a wavelength of 1557.3 nm. Details on the production and physics of ultracold metastable gases can be found in Ref. [26]. The advantage of using a QDG for spectroscopy is the small ODT trap depth required to trap the gas, which minimizes systematic shifts. The ODT is kept shallow at a depth of about 1.3 μK, and after thermalization the temperature of the gas is approximately 0.2 μK. We apply a small homogeneous magnetic field in the ODT to maintain spin polarization of the gas, which is required to have a trap lifetime > 10 s. The small Zeeman shift is directly measured using rf transitions between the $2\,^3S_1$ $M_J = +1, 0, -1$ states with kHz accuracy and therefore does not provide a limitation for our experimental accuracy [5].

A schematic overview of the ODT and the metrology infrastructure is shown in Fig. 2. The probe beam is generated using a Coherent 899-21 Ti:sapphire laser with an output power of 0.4 W at 887 nm. During the measurements the wavelength is registered using a wave meter. Simultaneously, we use an erbium-doped fiber laser frequency comb that is stabilized using a GPS-controlled rubidium clock to create a beat-note with the probe laser [5]. Combining the wave meter data with the beat-note data provides the absolute frequency of the probe laser.

Additionally, we stabilize the Ti:sapphire laser frequency to the frequency comb using a proportional-integral control loop. We control the Ti:sapphire laser frequency by keeping the beat-note frequency constant and scanning the repetition rate of the frequency comb. Because of the relatively slow loop time of 30 ms of the proportional-integral control loop, our laser has a Gaussian line shape with an average FWHM of approximately 1 MHz, with an accuracy of < 5 kHz, during the measurements.

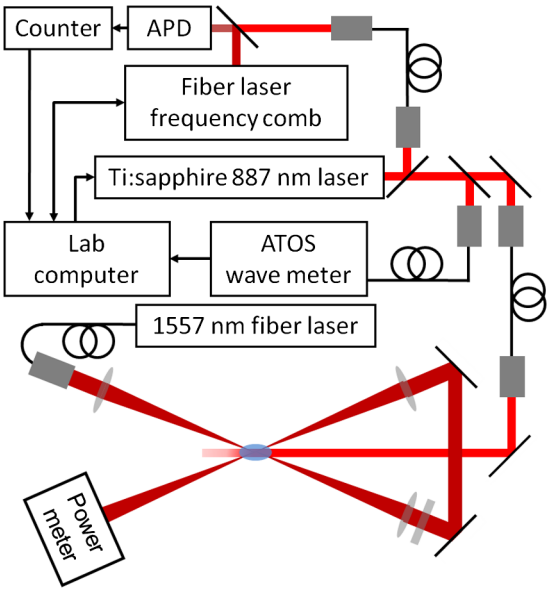

FIG. 2 (color online). Schematic overview of the setup. The crossed dipole trap is created using a fiber laser, and the trapping beam power is measured using a power meter. The spectroscopy light is generated using a Ti:sapphire ring laser. The beat-note between the spectroscopy laser and the frequency comb is measured with an avalanche photodiode (APD) connected to a frequency counter and digitally sent to the lab computer. The computer then calculates and sends a proportional-integral feedback signal to the Ti:sapphire laser to stabilize the spectroscopy laser frequency. The lab computer also interfaces with the frequency comb, enabling us to register and control the frequency comb settings.

In our experiment we measure a line scan over the resonance using 90 individual measurements with a frequency interval of 20 MHz. For every individual measurement, a new QDG sample has to be produced. Once the QDG is loaded in the ODT, an approximately 50 mW probe beam excites the atoms to the $2\,^1P_1$ state during 1 s. The excited atoms decay in 0.5 ns to the $1\,^1S_0$ state and leave the trap. Then the ODT is turned off and the remaining atoms fall due to gravity and hit a microchannel-plate (MCP) detector. The MCP current is measured to determine the TOF distribution of the atoms. This TOF distribution is fit using a bimodal distribution, which describes the momentum distribution of the BEC and thermal fractions. From the fit we obtain the atom number of both fractions, the temperature of the thermal fraction, and the chemical potential of the BEC [5]. Having measured the remaining total number of atoms at all 90

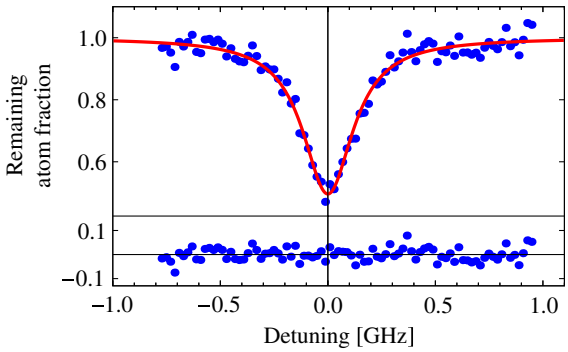

FIG. 3 (color online). Example of a single line scan measurement, showing 90 consecutive measurements over a range of approximately 1.8 GHz. A Lorentzian fit is used to determine the transition frequency and the linewidth. The residuals are shown in the lower plot. The frequency axis is centered on the transition frequency determined in this scan.

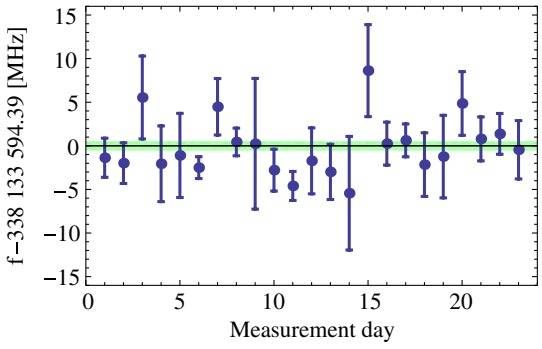

FIG. 4 (color online). Determined transition frequency averaged per measurement day, based on a total of 77 measurements. The error bars on the data represent the 1σ standard deviation of the daily average. The frequencies are centered around the final average transition frequency and the green bar represents its 1σ standard deviation of 0.5 MHz.

points, we can construct a normalized loss profile as seen in Fig. 3. The normalization is based on the remaining atom number after each individual measurement normalized by the far off-resonance remaining atom number of the line scan measurement. A fit with a Lorentzian line shape function is then used to obtain the linewidth and the central frequency [27].

The advantage of doing spectroscopy of a QDG in an ODT is the high degree of control over systematic effects. *Ab initio* calculations of the polarizabilities of both the $2\,^3S_1$ and $2\,^1P_1$ states at both the wavelength of the ODT and the spectroscopy beam are combined with previously performed ac Stark shift measurements [5]. The resulting ac Stark shift of the measured transition is 31 kHz. This is calculated with a few kHz precision as a result of the uncertainties in the laser beam intensity of the ODT. The Zeeman shift is measured to kHz precision as well. The recoil shift is 63.5 kHz, calculated with sub-kHz accuracy. Broadening effects due to the finite size of the QDG in the ODT and due to the momentum distribution of the gas [28] are below 50 kHz and therefore negligible as well. The mean-field shift cannot be calculated directly as the $2\,^3S_1 - 2\,^1P_1$ cold-collision scattering length is not known. However, the range of possible mean-field shifts can be calculated based on a model of Kokkelmans *et al.* [29] and the known ${}^5\Sigma_g^+$ $2\,^3S_1 - 2\,^3S_1$ scattering length of 142.0 (1) a_0, where a_0 is the Bohr radius [30]. From this model we find a worst-case mean-field shift of 90 kHz at extraordinary large scattering lengths [27]. However, the actual mean-field shift is expected to be much smaller as the finite lifetime of the $2\,^1P_1$ state reduces the mean-field interaction [31].

Based on a total of 77 line scans taken over a period of two months in the summer of 2013, the daily average transition frequency is shown in Fig. 4. We obtain a $2\,^3S_1 \rightarrow 2\,^1P_1$ transition frequency of 338 133 594.4 (0.5) MHz. This value is in good agreement with the most recent theoretical value of 338 133 594.9 (2.7) MHz [18], where the accuracy is limited by the QED calculations of the $2\,^3S_1$ state.

From our previously measured $2\,^3S_1 \rightarrow 2\,^1S_0$ transition frequency [192 510 702.1456 (0.0018) MHz [5]], we extract a $2\,^1S_0 \rightarrow 2\,^1P_1$ transition frequency of 145 622 892.2 (0.5) MHz. This result agrees with the recent $2\,^1S_0 \rightarrow 2\,^1P_1$ frequency measurement [20] within 0.6 (0.6) MHz. The $2\,^3S_1$ IE of 1 152 842 742.97 (0.06) MHz, derived from a measurement of the $2\,^3S_1 \rightarrow 3\,^3D_1$ transition frequency [13] and the calculated $3\,^3D_1$ IE [32], can now be combined with our result to give a $2\,^1P_1$ IE of 814 709 148.6 (0.5) MHz. Comparing this result to both measurements of Luo *et al.* [20,21], we find very good agreement. An overview of the most accurate experimental results and the QED calculations for the $2\,^1P_1$ IE is shown in Fig. 5. A discrepancy of $> 3\sigma$ with the theoretical IE as calculated by Yerokhin and Pachucki [18] remains. As QED calculations of most low-lying states of ^{4}He agree very well with experiment, improved calculations for the $2\,^1P_1$ state are

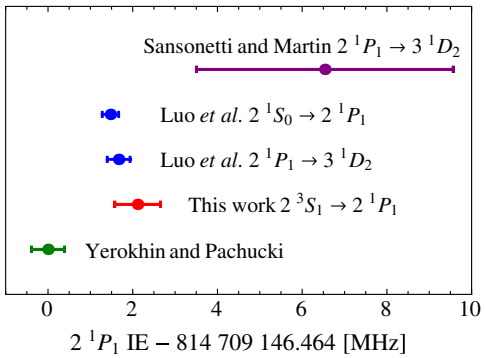

FIG. 5 (color online). Comparison of our experimental result for the $2\,^1P_1$ IE with other experiments [19–21] and QED theory by Yerokhin and Pachucki [18]. All recent experimental results show a $> 3\sigma$ discrepancy with theory.

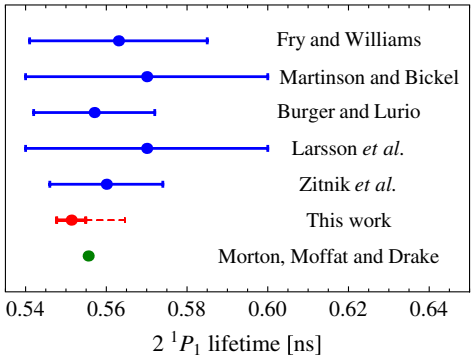

FIG. 6 (color online). Previously experimentally determined (blue) $2\,^1P_1$ lifetimes [23] compared to (red) our result and (green) the theoretical result by Morton, Moffat, and Drake [22]. Our result contains an extended, dashed, error bar indicating a systematic uncertainty as discussed in the text.

now timely. It may be that the contribution of $m\alpha^7$ terms is not treated well in this case, as a reevaluation of these terms has shifted the IE by almost 1 MHz [16,18].

The fit of our measurements to a Lorentzian line profile also provides the linewidth of the $2\,^1P_1$ state, which is among the largest of all atomic transitions in nature. Because of the finite number of atoms in the trap, the line shape of the trap loss signal is broadened as, even for an off-resonance laser beam, the number of atoms left in the trap will be zero for infinite interaction time. Therefore, we calculate the population of the $2\,^3S_1$ state using a three-level ($2\,^3S_1$, $2\,^1P_1$, and $1\,^1S_0$ states) optical Bloch equations model based on the model used by van Leeuwen and Vassen [33]. These equations can be solved analytically, and using the experimental parameters, we can determine the population of the $2\,^3S_1$ state as a function of the detuning of the spectroscopy beam. This calculated line shape allows us to correct for the aforementioned broadening effect [27].

Saturation of the MCP detector can lead to a broadening effect at the 1 MHz level of accuracy at which we determine the linewidth. Although saturation effects are expected and have been observed in other experiments with metastable helium BECs [34], analysis of our data shows no statistically significant broadening due to saturation. A systematic uncertainty is added to the result to indicate the worst-case shift in the linewidth if we allow a nonlinear response of the MCP detector in our analysis [27].

Based on the same 77 line scans from which we determine the transition frequency, we find a natural linewidth of $289\,(2)_{\mathrm{stat}}\,(^{+0}_{-7})_{\mathrm{syst}}$ MHz. This corresponds to a lifetime of the $2\,^1P_1$ state of $0.551\,(0.004)_{\mathrm{stat}}\,(^{+0.013}_{-0.000})_{\mathrm{syst}}$ ns. This result is shown in Fig. 6 together with previously determined lifetimes [23] and shows an improvement in the accuracy compared to the previous most accurate result. Our result is in agreement with the previous measurements, which are all based on completely different techniques, and agrees with a theoretical lifetime of 0.5555 ns, which is accurate to the last digit and calculated neglecting finite mass and relativistic effects that are expected below the 0.1% accuracy level [22].

To summarize, we have measured the $2\,^3S_1 \rightarrow 2\,^1P_1$ transition frequency in a quantum degenerate gas of $^4\mathrm{He}^*$ to 1.6×10^{-9} relative accuracy. From this measurement the $2\,^1P_1$ IE is determined with 6.7×10^{-10} relative accuracy, in agreement with two recent independent determinations by Luo *et al.* [20,21]. We show a $> 3\sigma$ discrepancy in the $2\,^1P_1$ IE with the most accurate QED calculation by Yerokhin and Pachucki [18], indicating that a renewed effort on the QED calculations is required. We also report the most accurate determination of the $2\,^1P_1$ lifetime to date. This new determination is in agreement with theory and all previous experimental determinations.

We acknowledge the Foundation for Fundamental Research on Matter (FOM) for financial support through the program "Broken Mirrors and Drifting Constants." We gratefully acknowledge K. S. E. Eikema for providing the use of the frequency comb and its infrastructure. We also would like to thank J. S. Borbely, S. Knoop, J. C. J. Koelemeij, S. J. J. F. M. Kokkelmans, and R. J. Rengelink for fruitful discussions and helpful suggestions.

*w.vassen@vu.nl

[1] T. Aoyama, M. Hayakawa, T. Kinoshita, and M. Nio, Phys. Rev. Lett. **109**, 111807 (2012).
[2] D. Hanneke, S. Fogwell, and G. Gabrielse, Phys. Rev. Lett. **100**, 120801 (2008).
[3] F. Biraben, Eur. Phys. J. Spec. Top. **172**, 109 (2009).
[4] A. Antognini *et al.*, Science **339**, 417 (2013).
[5] R. van Rooij, J. S. Borbely, J. Simonet, M. D. Hoogerland, K. S. E. Eikema, R. A. Rozendaal, and W. Vassen, Science **333**, 196 (2011).
[6] S. Sturm, F. Köhler, J. Zatorski, A. Wagner, Z. Harman, G. Werth, W. Quint, C. H. Keitel, and K. Blaum, Nature (London) **506**, 467 (2014).
[7] R. Pohl, R. Gilman, G. A. Miller, and K. Pachucki, Annu. Rev. Nucl. Part. Sci. **63**, 175 (2013).
[8] P. Cancio Pastor, L. Consolino, G. Giusfredi, P. De Natale, M. Inguscio, V. A. Yerokhin, and K. Pachucki, Phys. Rev. Lett. **108**, 143001 (2012).
[9] T. Nebel *et al.*, Hyperfine Interact. **212**, 195 (2012).
[10] C. T. Chantler *et al.*, Phys. Rev. Lett. **109**, 153001 (2012).
[11] W. Lichten, D. Shiner, and Z.-X. Zhou, Phys. Rev. A **43**, 1663 (1991).
[12] C. J. Sansonetti and J. D. Gillaspy, Phys. Rev. A **45**, R1 (1992).
[13] C. Dorrer, F. Nez, B. de Beauvoir, L. Julien, and F. Biraben, Phys. Rev. Lett. **78**, 3658 (1997).
[14] P. Cancio Pastor, G. Giusfredi, P. De Natale, G. Hagel, C. de Mauro, and M. Inguscio, Phys. Rev. Lett. **92**, 023001 (2004).
[15] D. Z. Kandula, C. Gohle, T. J. Pinkert, W. Ubachs, and K. S. E. Eikema, Phys. Rev. Lett. **105**, 063001 (2010).

[16] K. Pachucki, Phys. Rev. A **74**, 062510 (2006); **76**059906(E) (2007).
[17] G. W. F. Drake, and Z.-C. Yan, Can. J. Phys. **86**, 45 (2008).
[18] V. A. Yerokhin and K. Pachucki, Phys. Rev. A **81**, 022507 (2010).
[19] C. J. Sansonetti and W. C. Martin, Phys. Rev. A **29**, 159 (1984).
[20] P.-L. Luo, J.-L. Peng, J.-T. Shy, and L.-B. Wang, Phys. Rev. Lett. **111**, 013002 (2013); **111**179901(E) (2013).
[21] P.-L. Luo, Y.-C. Guan, J.-L. Peng, J.-T. Shy, and L.-B. Wang, Phys. Rev. A **88**, 054501 (2013).
[22] D. C. Morton, P. Moffat, and G. W. F. Drake, Can. J. Phys. **89**, 129 (2011).
[23] E. S. Fry and W. L. Williams, Phys. Rev. **183**, 81 (1969); I. Martinson and W. S. Bickel, Phys. Lett. **30A**, 524 (1969); J. M. Burger and A. Lurio, Phys. Rev. A **3**, 64 (1971); J. Larsson, E. Mevel, R. Zerne, A. L'Huillier, C.-G. Wahlström, and S. Svanberg, J. Phys. B **28**, L53 (1995); M. Žitnik, A. Stanič, K. Bučar, J. G. Lambourne, F. Penent, R. I. Hall, and P. Lablanquie, J. Phys. B **36**, 4175 (2003).
[24] G. W. F. Drake, Phys. Rev. **181**, 23 (1969).
[25] G. W. F. Drake and D. C. Morton, Astrophys. J. Suppl. Ser. **170**, 251 (2007).
[26] W. Vassen, C. Cohen-Tannoudji, M. Leduc, D. Boiron, C. I. Westbrook, A. Truscott, K. Baldwin, Gerhard Birkl, P. Cancio Pastor, and M. Trippenbach, Rev. Mod. Phys. **84**, 175 (2012).
[27] See Supplemental Material at http://link.aps.org/supplemental/10.1103/PhysRevLett.112.253002 for the calculations of these systematic effects.
[28] T. C. Killian, Phys. Rev. A **61**, 033611 (2000).
[29] S. J. J. M. F. Kokkelmans, B. J. Verhaar, K. Gibble, and D. J. Heinzen, Phys. Rev. A **56**, R4389 (1997).
[30] S. Moal, M. Portier, J. Kim, J. Dugué, U. D. Rapol, M. Leduc, and C. Cohen-Tannoudji, Phys. Rev. Lett. **96**, 023203 (2006).
[31] P. S. Julienne and F. H. Mies, J. Opt. Soc. Am. B **6**, 2257 (1989).
[32] G. W. F. Drake and W. C. Martin, Can. J. Phys. **76**, 679 (1998).
[33] K. A. H. van Leeuwen and W. Vassen, Europhys. Lett. **76**, 409 (2006).
[34] M. Schellekens, R. Hoppeler, A. Perrin, J. Viana Gomes, D. Boiron, A. Aspect, and C. I. Westbrook, Science **310**, 648 (2005).